Original Research

Single-Breathhold, Four-Dimensional, Quantitative Assessment of LV and RV Function Using Triggered, Real-Time, Steady-State Free Precession MRI in Heart Failure Patients

Girish Narayan, MD,[1]* Krishna Nayak, PhD,[2] John Pauly, PhD,[3] and Bob Hu, MD[2,4]

Purpose: To validate a novel, real-time, steady-state free precession (SSFP), single-breathhold technique for the assessment of left ventricular (LV) and right ventricular (RV) function in heart failure patients.

Materials and Methods: A total of 20 heart failure patients (mean age 59 ± 17 years) underwent scanning with our new, real-time, spiral SSFP sequence in which each cardiac phase was acquired in 118 msec at a resolution of 1.8 × 1.8 mm. Each cardiac slice (1-cm thick) was automatically advanced based on a cardiac trigger, allowing complete coverage of the heart in a single breathhold. The patients also underwent LV and RV assessment with the gold standard: multiple breathhold, cardiac-gated, segmented k-space strategy. LV and RV end-systolic volume (ESV) and end-diastolic volume (EDV) and LV mass were compared between the two imaging techniques.

Results: The new real-time strategy was highly concordant with the gold standard technique in the assessment of LVEDV (r = 0.98), LVESV (r = 0.98), RVESV (r = 0.86), RVEDV (r = 0.91), LVMASS (r = 0.95), RVEF (r = 0.70), and LVEF (r = 0.94). The mean bias (95% confidence interval [CI]) for each parameter is LVEDV: 10.6 cc (cm^3) (3.8–17.4 cc), LVESV: –0.8 cc (–5.3 to 3.7 cc), RVEDV: 3.7 cc (–5.6 to 13.2 cc), RVESV: –3.1 cc (–11.1 to 4.9 cc), LVMASS: 26 g (12.4–39.8 g), RVEF: –2.9% (1.3 to –7.2 %), LVEF: 1.9% (5 to –1.1%). In addition, data acquisition was only nine ± two seconds with the real-time strategy vs. 312 ± 41 seconds for the standard technique.

Conclusion: In patients with heart failure, real-time, spiral SSFP allows rapid and accurate assessment of RV and LV function in a single-breath hold. Using the same strategy, increased temporal resolution will allow real-time assessment of cardiac wall motion during stress studies.

Key Words: MRI; imaging; heart failure; SSFP; spirals
J. Magn. Reson. Imaging 2005;22:59–66.

ACCURATE AND REPRODUCIBLE assessment of cardiac function and chamber volume is vital to the care of heart failure patients (1). However, exact ventricular volumes and mass are not routinely obtained even in settings in which quantitative data is useful, partly due to the measurement inaccuracy of established modalities such as echocardiography (2,3). While previous authors have validated the accuracy of cardiac MRI–derived volume and functional data (4), existing strategies suffer from measurement variability and decreased clinical robustness in heart failure patients (5), Current techniques require ill, dyspneic patients to undertake multiple, prolonged breathholds in the exact same diaphragmatic position. They also collect and assemble data over multiple cardiac cycles, causing image degradation during arrhythmias. In addition, the process of complete volumetric imaging of the entire right ventricle (RV) and left ventricle (LV) can take as long as 10–15 minutes, during which time patient motion will compromise image quality and quantitative accuracy. Current techniques are thus ill-suited for routine application in heart failure patients and have hampered the clinical utility of cardiac MRI.

Recently, steady-state free precession (SSFP) sequences have been introduced to cardiac MR imaging (6). While its increased signal to noise ratio and blood-myocardial contrast has improved image quality, the quantitation of cardiac function continues to suffer from prolonged image acquisition times and the need for multiple breathholds. Its incorporation in faster, real-time imaging strategies has been hampered by the relative inefficiency of k-space sampling techniques, with resultant poor temporal and spatial resolution (7,8). Some investigators have advocated combining real-time techniques with a free-breathing strategy to as-

[1]Division of Cardiovascular Medicine, Stanford University Hospital, Stanford, California, USA.
[2]Department of Electrical Engineering, University of Southern California, California, USA.
[3]Department of Electrical Engineering, Stanford University, Stanford, California, USA.
[4]Division of Cardiology, Palo Alto Medical Foundation, Palo Alto, California, USA.
Contract grant sponsor: National Institutes of Health; Contract grant number: R01HL067161.
Presented in part at the ISMRM meeting, Kyoto, Japan, 2004, for 2nd Place Poster Award.
Supplementary material for this article can be found on the JMRI website at: www.interscience.wiley.com/jpages/1053-1807/suppmat/index.html.
*Address reprint requests to: G.N., 300 Pasteur Drive, CVRB, Stanford, CA 94305. E-mail: gnarayan@stanford.edu
Received July 29, 2004; Accepted March 31, 2005.
DOI 10.1002/jmri.20358
Published online in Wiley InterScience (www.interscience.wiley.com).

Table 1
Sequence Comparison

Basis	Standard SSFP	Real-time SSFP
k-space coverage	Segmented, Cartesian 192 × 192 matrix	Spiral, 20 interleaves
Slice advancement	Multiple breathhold	Cardiac triggered
FOV	35 × 35 cm	20 × 20 cm
Spatial resolution	1.8 × 1.8 mm	1.8 × 1.8 mm
Temporal resolution	60 msec/segment[a]	118 msec/slice/phase (42 msec)[b]
TR/TE	3.7 msec/1.6 msec	5.9 msec/2.2 msec
ST/SP	10/0 mm	10/0 mm
Flip angle	40 degrees	40 degrees
Other		Adjustable phase[c]

[a]Using view-sharing.
[b]Intermediate temporal phase was displayed using sliding window reconstruction.
[c]Phase at the flip angle could be interactively adjusted to move banding artifacts outside the region of interest.

sess LV and RV volumes quantitatively. However, free-breathing strategies are prone to slice misregistration errors and may compromise interstudy reproducibility. We have recently described a new high-resolution spiral sequence that provides efficient k-space sampling for real-time imaging with SSFP (9). This strategy provides complete coverage of RV and LV function in a single breathhold by employing a multislice strategy in which one slice is imaged every heartbeat (10). This single-breathhold strategy was assessed in 20 patients with congestive heart failure and validated with the gold standard: gated, segmented k-space, multiple breathhold acquisition.

MATERIALS AND METHODS

Pulse Sequences

Triggered, Real-Time, SSFP Sequence

The standard and comparison sequences are summarized in Table 1. A full technical description of the real-time sequence is provided elsewhere (9). The main details of the pulse sequence is shown in Fig. 1. A real-time, refocused, spiral SSFP sequence was implemented with a 640 μs slice-selective excitation pulse followed by 2.4 msec spiral readouts with M0 and M1 (zero and first moment) refocusing gradients, and a 1.4-msec rewinder. Using an imaging TR of 5.9 msec and 20 interleaves, spatial resolution of 1.8 × 1.8 mm was achieved over a 20-cm field of view (FOV) every 118 msec. Sliding window reconstruction was used to display intermediate temporal phase at 24 frames/second (every 42 msec). Slice thickness was 10 mm with no interslice gap. As SSFP is highly sensitive to off-resonance, radiofrequency (RF) phase cycling could be interactively adjusted using the real-time user interface to place SSFP banding outside the region of interest (9).

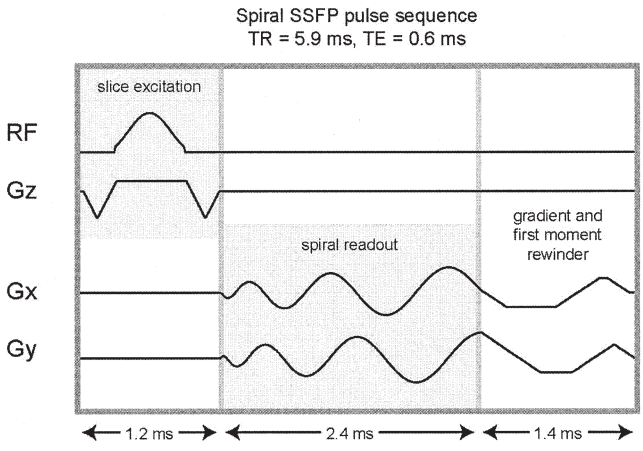

Figure 1. Diagram of spiral, refocused, SSFP sequence; 1.2 msec excitation (640 μs of RF), 2.4 msec readout, 1.4 msec rewinder (for zero and first moment).

Standard SSFP Sequence

A cardiac-gated, segmented k-space, SSFP sequence ((FIESTA), GE Medical Systems, Milwaukee, WI, USA) was used as the standard comparison sequence. Sequence details are provided in Table 1. Multiple slices were prescribed from base to apex. Each slice was acquired consecutively during a 15–20-second breathhold.

Imaging Protocol

All studies were performed in a GE Signa 1.5-T scanner (GE Medical Systems, Milwaukee, WI, USA) equipped with the Stanford real-time interactive (RTI) system (11) The scanner was equipped with gradients supporting a magnitude of 40 mT/m and slew rate of 150 T/m/second. A five-inch surface coil was used as a receiver in all studies.

A total of 20 patients (mean age 59 ± 17 years, 13 men, and seven women) with a history of clinical heart failure were recruited from heart failure clinics. Informed consent was obtained for all subjects in accordance with our institutional review board. The primary diagnoses of the patients were idiopathic dilated cardiomyopathy ($N = 4$), ischemic heart disease ($N = 7$), moderate to severe mitral regurgitation ($N = 2$), primary pulmonary hypertension ($N = 2$), pulmonary regurgitation ($N = 1$), hypertrophic cardiomyopathy ($N = 1$), combined pulmonary and aortic insufficiency ($N = 1$), and hypertensive disease ($N = 2$). Each underwent scanning with the standard and new (triggered, real-time spiral SSFP) sequence using the protocol described below.

The standard sequence was used to obtain multiple, consecutive slices from the base to the apex of the left

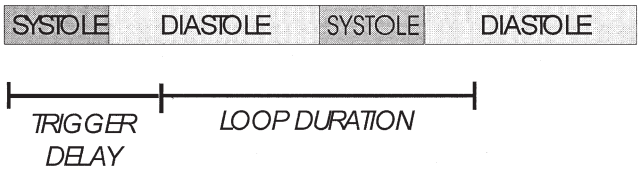

Figure 2. Desired selection of the trigger delay to delineate the end-diastolic and end-systolic phases, while avoiding the steady-state transition.

ventricle. After the standard sequence was completed, the real-time sequence was initiated. Short-axis views were localized in real-time. Phase cycling was adjusted to optimize image quality. The exact position of the basal slice obtained on the standard sequence was localized in real-time, with fine adjustments made during the breath-hold. After the requested breathhold, the sequence was switched to a "triggered" mode, in which each slice was acquired and automatically advanced based on a cardiac trigger. The trigger delay was adjusted to ensure adequate delineation of the end-diastolic and end-systolic phases of the cardiac cycle (see Fig. 2). In addition, slice advancement was halted for short RR intervals, (defined as less than 75% of the basal RR interval). This prevented slice advancement after premature beats. All acquisition was performed during continuous scanning. The total number of slices was adjusted based on the size of the heart. Generally, 8–12 slices could be obtained in a breathhold lasting 8–12 RR intervals. Each time a slice location was shifted, remaining magnetization of the old slice was spoiled. For both sequences, breathholding was performed in end-expiration. Both sequences were performed on the same day.

Image Analysis

To determine the accuracy of RV and LV volume assessment, we calculated parameters for both techniques. Manual segmentation of the LV and RV end-diastolic and end-systolic endocardial surfaces and LV end-diastolic epicardial surface was completed off-line using the MASS software package (Medis Inc., Leiden, the Netherlands) for the standard sequence images and Scion Image (Scion Corp., Frederick, MD, USA) for the real-time images. Two separate packages were used, as neither package could handle both data sources. Calculation of volumes of phantoms imaged with both techniques demonstrates excellent agreement when analyzed by the two packages (data not shown). The papillary muscles were not included in the analysis. The basal section of the LV was defined as the slice at which at least 50% of the LV myocardial circumference was visible in all cardiac phases. The basal diastolic and systolic slice of the RV was the first slice not to include any part of the RV outflow tract. The exact starting slice position used in the standard sequence was obtained by real-time adjustment of the plane while using the new, comparison sequence. This ensured similar basal slice positioning between the two sequences and minimized error resulting from disparate slice correspondence between the two sequences. End-diastolic volume (EDV) and end-systolic volume (ESV) were calculated by summing the area determined in each slice multiplied by the slice thickness. LV mass (LVMASS) was calculated using the difference between the end-diastolic epicardial versus endocardial volumes multiplied by the density of the myocardium (1.05 g/cm^3). Datasets were reviewed after a period of at least two weeks by the same individual and by a different individual experienced in cardiac MR to obtain intra- and interobserver variability.

Statistical Evaluation

Quantitative values of LVEDV, LVESV, RVEDV, RVESV, and LVMASS were compared between the standard technique and the triggered, real-time, SSFP technique using correlation analysis. Bland-Altman (12) analysis was performed to assess for any systematic differences between the two techniques. Intra- and interobserver variability was calculated as the percentage of the absolute difference between the measurements divided by the mean of the two measurements.

RESULTS

Accuracy of Volumetric Measurements

Representative movie clips and still frames of the short-axis view obtained using our triggered, real-time, SSFP sequence in a patient with dilated cardiomyopathy and in a patient with RV enlargement demonstrate excellent blood-myocardial definition (Fig. 3; and Supplementary Movie (Supplementary material for this article can be found on the JMRI website at: www.interscience.wiley-.com/jpages/1053-1807/suppmat/index.html.). In all studies, satisfactory end-diastolic and end-systolic frames were obtained at each slice location to allow accurate border delineation for subsequent volume calculation. In the real-time images, upon each slice shift, there was a noticeable period during which the new slice reached steady state. This did not interfere with the assessment of function or volume as the trigger delay was adjusted to place the relevant end-diastolic and end-systolic frames outside this transient period.

There was excellent agreement between the standard sequence and the triggered, real-time, SSFP approach for volumetric and functional assessments (see Fig. 4; left). The results of the Bland-Altman analysis are shown in Fig. 4 (right). The assessments of LVEDV and LVMASS obtained with the triggered, real-time approach were 10.6 ± 3.2 cc (cm^3) and 26 ± 6.8 g (mean $\pm$ SD) higher than those obtained using the standard sequence ($P < 0.05$). However, the other parameters showed no statistically significant evidence of systematic difference. Inter- and intraobserver variability are presented in Table 2.

Time Efficiency

All patients were able to complete the required protocol. The mean scan time for complete volumetric coverage of the heart after short axis localization was nine $\pm$ two seconds for the real-time vs. 312 ± 41 seconds for the standard approach. The latter time included recovery

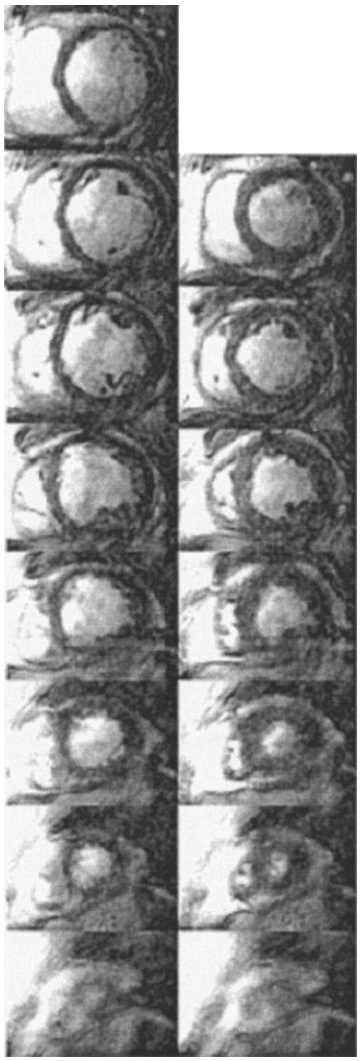

Figure 3. End-diastolic (left) and end-systolic (right) frames from a patient with dilated cardiomyopathy acquired in a single breathhold from base to apex using the new triggered, real-time, SSFP sequence.

time between breathholds as deemed necessary by the patient. Heart rates ranged from 53 to 93 beats per minute, resulting in a single breathhold duration for the real-time approach of seven to 15 seconds as compared to eight to 12 breathholds of 15 to 20 seconds each for the standard sequence.

DISCUSSION

We have demonstrated that, in a single breathhold, LV and RV function and volumes can be accurately quantified in heart failure patients with a real-time, spiral SSFP sequence.

Currently, the common clinical approach for this purpose includes CINE MR techniques, which are based on cardiac gated, multiphase, segmented k-space sequences, in which every slice acquisition requires a breathhold (13–15). However, the requirement for multiple breathholds and the need to combine data from multiple cardiac cycles complicates clinical scans in patients with dyspnea and arrhythmias, characteristics present in the heart failure population (1). In addition, these strategies, as currently implemented, require a prescription phase during which scan planes are identified, followed after a length of time by the actual scans. This strategy has the potential to introduce patient motion related positioning errors and also extends overall scan time. As the study represents only a part of the cardiac examination, patients often complain of excessive overall study duration.

In order to address these limitations, real-time techniques, in which cardiac motion is captured without the need for gating, allows an interactive, rapid cardiac examination and has proven useful for the assessment of ventricular volumes (11,16–19,20). However, these previous real-time techniques were based on gradient recalled echo sequences, which primarily rely on T1 and in-flow to produce contrast. In comparison, SSFP techniques produce enhanced endocardial-blood contrast as a result of its T2 and T1 dependence and effective use of all available signal. As a result, it has been widely adopted for rapid cine imaging of the heart.

We have combined the inherently high blood-myocardial contrast characteristics of SSFP sequences with the advantages of the real-time approach. Other authors have also described the use of SSFP for real-time imaging (7,8). However, Hori et al (7), employed the relatively less efficient two-dimensional Fourier transform (FT) strategy with a resulting true temporal resolution of 164 msec and a spatial resolution of 4.17 $\times$ 2.73 mm. Spuentrup et al (8) achieved a higher spatial resolution of 2.5 $\times$ 2.5 mm, though at a much lower true temporal resolution of 200 msec. In addition, their use of projection reconstruction grossly undersamples k-space data. In comparison, using spiral k-space trajectories, we have achieved a true temporal resolution of 118 msec and 1.8 $\times$ 1.8 mm resolution without any undersampling. The improved temporal and spatial resolution will better delineate cardiac borders, especially during the rapidly occurring systolic phase (19). Temporal resolutions of approximately 90 msec have previously been shown to demonstrate good volumetric assessment during end-systole and end-diastole. Our temporal resolution (118 msec) is close to this value. Furthermore, Foo et al (21) demonstrated that the use of the intermediate temporal phase is important in improving the temporal characteristics of the sequence. The use of the sliding window reconstruction technique, in our technique, provides 24 images per second. Finally, the performance of the sequence demonstrates close agreement of the quantitative values to the gold standard values obtained in our study.

Overall, our technique yielded very accurate and reproducible values for LV and RV volumes as compared to the standard technique. In this study, the LVEDV and LVMASS were larger than the values determined by the standard technique by 6.6% ($P < 0.05$) and 13% ($P < 0.05$), respectively. In addition, the RVEDV showed a trend toward being larger ($P < 0.07$) as compared to the gold standard acquisition. This leads us to speculate that the multiple breathhold sequence may introduce systematic errors due to changes in expiratory position and resulting slice misregistration.

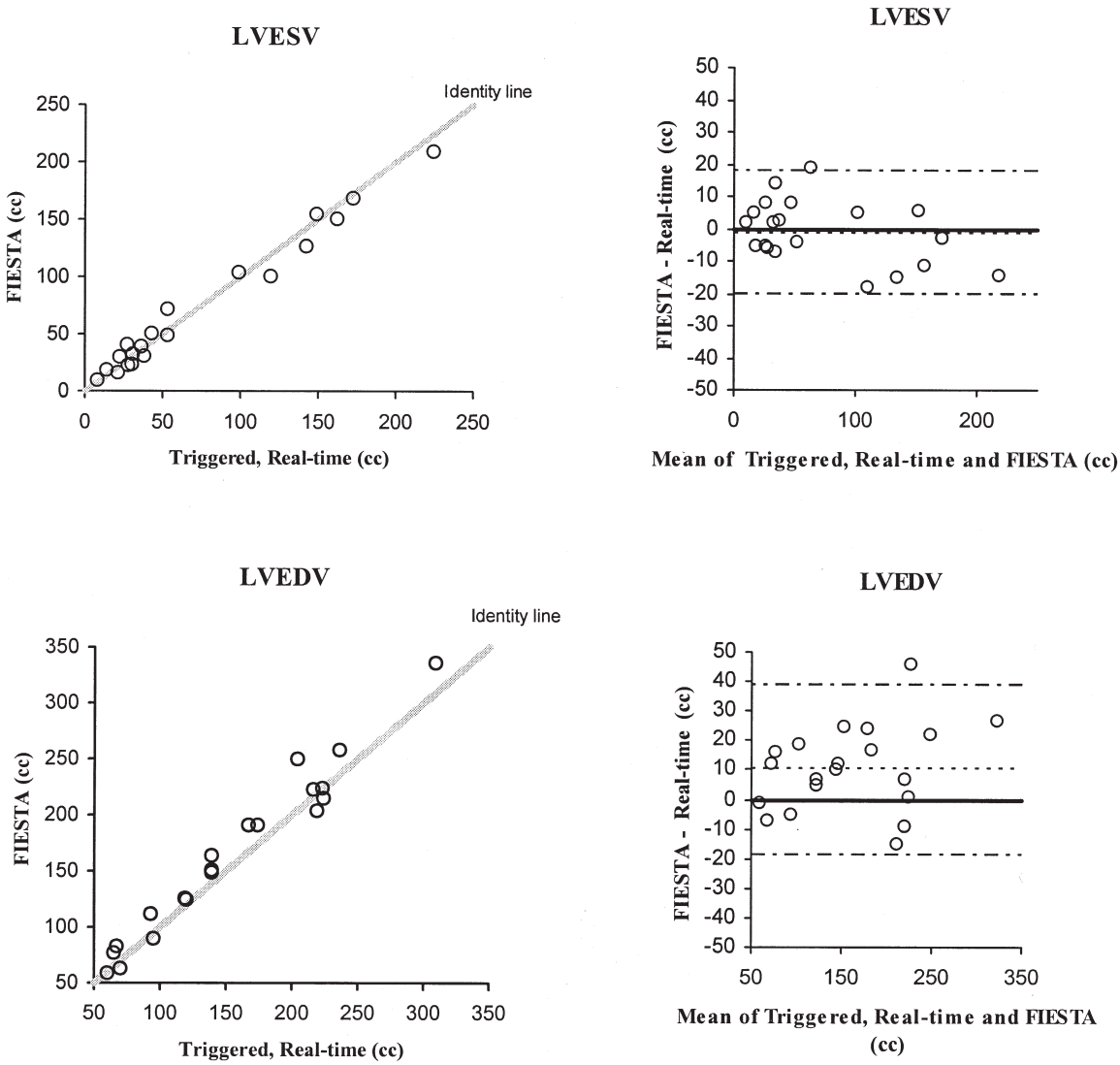

Figure 4. Correlation of FIESTA and triggered, real-time (left) and bias plot (right). The correlation coefficients are LVESV: r = 0.98; LVEDV: r = 0.98; RVESV: r = 0.86; RVEDV: r = 0.91; LVMASS: r = 0.95, RVEF: r = 0.70; and LVEF: r = 0.94. The mean bias is represented by the dotted line. The dashed lines indicate the 95% limits of agreement. The solid line indicates zero bias. The mean bias (95% CI) for each parameter is LVEDV: 10.6 cc (3.8–17.4 cc); LVESV: –0.8 cc (–5.3 to 3.7 cc); RVEDV: 3.7 cc (–5.6 to 13.2 cc); RVESV: –3.1 cc (–11.1 to 4.9 cc); LVMASS: 26 g (12.4–39.8 g); RVEF: –2.9% (1.3 to –7.2 %); and LVEF: 1.9% (5 to –1.1%).

The use of the SSFP sequence also introduces transient artifacts, which result from steady-state discontinuity when a new slice is imaged. In theory, this may interfere with the interpretation of cardiac function. However, in patients, we have found that the duration of this artifact is small. Furthermore, the trigger delay is optimally adjusted to prevent this transient artifact from interfering with the end-diastolic phase. Further shortening of the transients may be possible with advanced steady-state methods as described by Hargreaves et al (22).

In addition, our values for inter- and intraobserver variability are similar to those described in the literature for assessments of diastolic and systolic LV and RV volumes (7,17,19). The values between the standard and the real-time approach are also quite similar, suggesting that both techniques offer adequate image quality to render reproducible interpretations.

Overall scan time is also decreased using our strategy. The use of a triggered, spiral, real-time approach allows complete volumetric coverage of the right and left ventricles in a single breathhold. This approach also obviates the need for a prolonged localizer step, with interactive scanning and position occurring in real-time. This dramatically reduces scan time (by an average of about five minutes in our study, not including scout image acquisition used in conventional techniques) compared to the standard sequence. In addition, patient motion does not require repeating the localization and prescription scans.

Our strategy also decreases the overall breathhold requirements for patients. We have also coupled real-time techniques with free breathing strategies (17). However, these require exquisite correlation with diaphragm position in order to minimize slice misregistra-

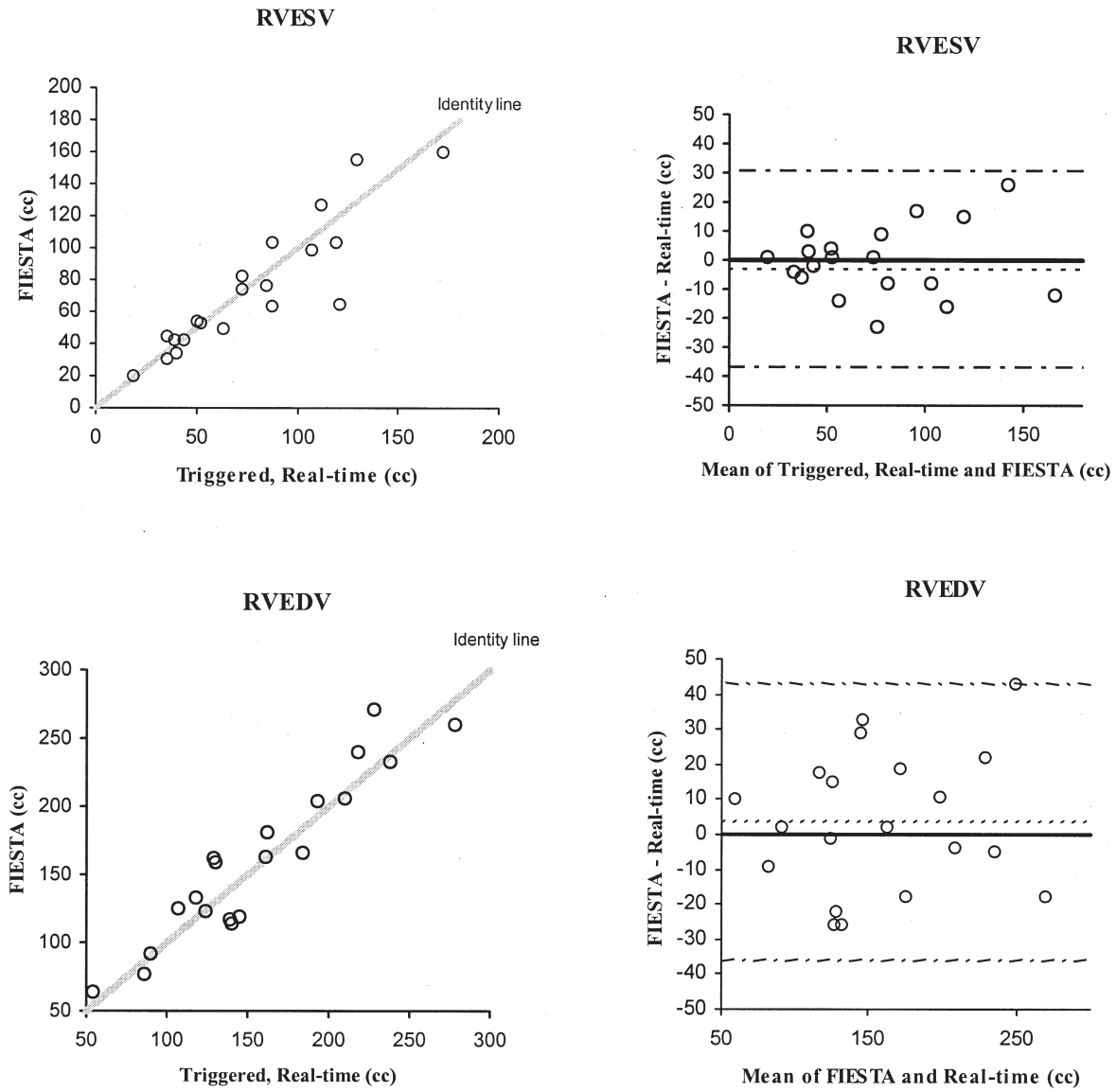

Figure 4 (Continued)

tion given respiratory related changes in cardiac position and ventricular volume. As a result, these techniques may suffer from poor interstudy reproducibility, depend heavily on operator expertise, and thus lack clinical robustness compared to breathheld scans. Furthermore, cardiac MR has been proposed as the technique of choice to assess treatment effects in clinical studies given its accuracy, low interobserver variability, and subsequent potential to dramatically reduce sample size (23). However, the changes in ejection fraction observed in clinical studies, often on the order of 8% to 10% (24), require a technique that has low interstudy variability as well (5). By adopting a single-breathhold strategy, one can eliminate possible error introduced by slice-to-slice variation in diaphragm position and resulting slice misregistration. This also serves to decrease operator and patient dependence, at the same time minimizing patient breathholds. Given that most patients, including those with heart failure, can hold their breath once for at least 10 seconds, a single breathhold strategy promises to provide clinically more robust results. Further assessment of interstudy variability using this technique in a larger group of patients would quantitate this benefit.

Arrhythmias are also frequently present in the heart failure population (i.e., ventricular bigeminy, premature ventricular contradiction (PVCs), atrial fibrillation, etc.) During a segmented k-space approach, the presence of these arrhythmias will frustrate efficient, high-quality image acquisition. While collection of this data over multiple heartbeats may serve to "average" data over multiple samples, true real-time wall motion is not depicted. Furthermore, it remains unclear whether the accuracy of this approach will be superior to averaging multiple single-volumetric acquisitions using our strategy. Taken to the extreme, standard techniques of "averaging" over multiple cardiac cycles could lead to a "static" movie of the heart by averaging many possible positions of the myocardium. In our strategy, during real-time imaging, each phase is visualized in real-time,

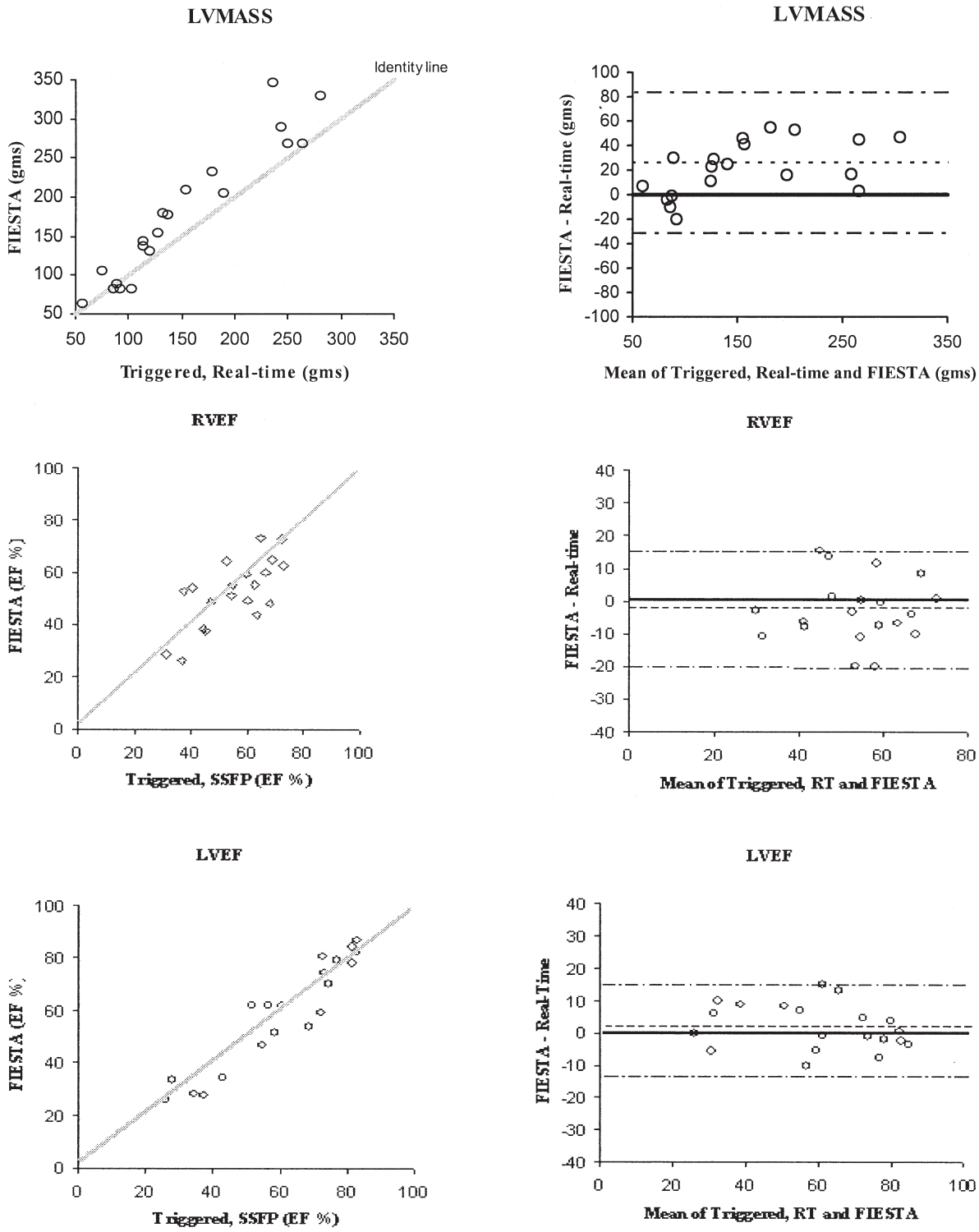

Figure 4 (Continued

removing the requirement for a regular rhythm. For volumetric calculations, rejection of short RR intervals, where the slice was not advanced, may capture a slice during postextrasystolic augmentation, thus not reflecting true basal LV function. However, the error introduced by this is confined to that one slice. Furthermore, in patients with frequent ectopy, multiple acquisitions of the entire cardiac volume can be obtained very quickly, allowing one to average over multiple samples. Nonetheless, further study will be needed in this regard to quantify the benefit of this strategy in a larger cohort of patients with arrhythmias.

In this study, primary emphasis was placed on the assessment of ventricular volumes. Though we believe that accurate wall motion analysis is also obtained in an analogous rapid fashion, a larger patient cohort with

Table 2
Intra- and Interobserver Variability*

	LVEDV	LVESV	RVEDV	RVESV	LVMASS
Intraobserver variability					
Triggered	5.6 ± 4.5	9.2 ± 5.3	7.9 ± 3.9	7.4 ± 4.1	10.5 ± 2.1
Fiesta	5.8 ± 4.1	8.8 ± 6.2	10.1 ± 5.7	12.1 ± 4.9	8.5 ± 4.9
Interobserver variability					
Triggered	5.3 ± 2.9	15.0 ± 2.4	4.5 ± 0.8	8.2 ± 9.5	13 ± 6.5
Fiesta	4.4 ± 3.9	13.5 ± 8.2	8.4 ± 7.0	16.3 ± 9.4	10.8 ± 8.5

*All values are expressed as percentages, calculated as the absolute difference of the two measurements divided by the mean ± SD.

a larger sample of regional wall motion abnormalities would be required to rigorously address this. In this regard, in contrast to segmented strategies, our strategy allows true depiction of wall motion in real-time. Parameter adjustment in our strategy to yield improved temporal resolution (at the expense of spatial resolution) promises to facilitate true real-time myocardial stress evaluation (25). In conclusion, triggered, real-time, spiral SSFP allows rapid and accurate quantitation of RV and LV function in patients with heart failure. This technique provides a clinically robust, rapid modality to accurately assess cardiac function in heart failure patients using cardiac MRI.

REFERENCES

1. Hunt SA, Baker DW, Chin MH, et al. ACC/AHA guidelines for the evaluation and management of chronic heart failure in the adult: a report of the American College of Cardiology/American Heart Association Task Force on Practice Guidelines (Committee to Revise the 1995 Guidelines for the Evaluation and Management of Heart Failure). 2001. American College of Cardiology Web site. Available at: http://www.acc.org/clinical/guidelines/failure/hf_index.htm.
2. Bottini PB, Carr AA, Prisant LM, et al. Magnetic resonance imaging compared to echocardiography to assess left ventricular mass in the hypertensive patient. Am J Hypertens 1995;8:221–228.
3. Teichholz LE, Kreulen T, Herman MV, et al. Problems in echocardiographic volume determinations: echocardiographic-angiographic correlations in the presence or absence of asynergy. Am J Cardiol 1976;37:7–11.
4. Bellenger NG, Grothues F, Smith G, et al. Quantification of right and left ventricular function with MRI. Herz 2000;25:392–399.
5. Grothues F, Smith GC, Moon JC, et al., Comparison of interstudy reproducibility of cardiovascular magnetic resonance with two-dimensional echocardiography in normal subjects and in patients with heart failure or left ventricular hypertrophy. Am J Cardiol 2002;90:29–34.
6. Thiele H, Nagel E, Paetsch I, et al. Functional cardiac MR imaging with steady-state free precession (SSFP) significantly improves endocardial border delineation without contrast agents. J Magn Reson Imaging 2001;14:362–367.
7. Hori Y, Yamada N, Higashi M, et al. Rapid evaluation of right and left ventricular function and mass using real-time true-FISP cine MR imaging without breath-hold: comparison with segmented true-FISP cine MR imaging with breath-hold, J Cardiovasc Magn Reson 2003;5:439–450.
8. Spuentrup E, Schroeder J, Mahnken AH, et al. Quantitative assessment of left ventricular function with interactive real-time spiral and radial MR imaging. Radiology 2003;227:870–876.
9. Nayak KS, Hargreaves B, Hu BS, et al., Spiral balanced SSFP cardiac imaging. Magn Reson Med 53:1468–1473.
10. Nayak K, Hu BS. Triggered real-time MRI and cardiac applications. Magn Reson Med 2003;49:188–192.
11. Kerr ABS, Li KCP, Handy CJ, Mayer CH, Macovski A, Nishimura DG. Real-time interactive MRI on a conventional scanner. Magn Reson Med 1997;38:355–367.
12. Bland JM, Altman DG. Statistical methods for assessing agreement between two methods of clinical measurement. Lancet 1986;1:307–310.
13. Buser PT, Aufermann W, Holt WW, et al. Noninvasive evaluation of global left ventricular function with use of cine nuclear magnetic resonance. J Am Coll Cardiol 1989;13:1294–1300.
14. Sakuma H, Fujita N, Foo TK, et al. Evaluation of left ventricular volume and mass with breath-hold cine MR imaging. Radiology 1993;188:377–380.
15. Sechtem U, Pfugfelder PW, Gould RG, et al. Measurement of right and left ventricular volumes in healthy individuals with cine MR imaging. Radiology 1987;163:697–702.
16. Yang PC, Karr AB, Liu AC, et al. New real-time interactive magnetic resonance imaging complements echocardiography. J Am Coll Cardiol 1998;32:2049–2056.
17. Kaji S, Yang PC, Kerr AB, et al. Rapid evaluation of left ventricular volume and mass without breath-holding using real-time interactive cardiac magnetic resonance imaging system. J Am Coll Cardiol 2001;38:527–533.
18. Nagel E, Schnieder U, Ibrahim T, et al. Magnetic resonance real-time imaging for the evaluation of left ventricular function. J Cardiovasc Magn Reson 2000;2:7–14.
19. Setser RM, Fischer SE, Lorenz CH. Quantification of left ventricular function with magnetic resonance images acquired in real time. J Magn Reson Imaging 2000;12:430–438.
20. Bornstedt A, Nagel E, Schalla S, et al. Multi-slice dynamic imaging: complete functional cardiac MR examination within 15 seconds. J Magn Reson Imaging 2001;14:300–305.
21. Foo TK, Bernstein MA, Aisen AM, et al. Improved ejection fraction and flow velocity estimates with use of view-sharing and uniform repetition time excitation with fast cardiac techniques. Radiology 1995;195:471–478.
22. Hargreaves BA, Vasanawalla SS, Pauly JM, et al. Characterization and reduction of the transient stead-state in MR imaging. Magn Reson Med 2001;46:149–153.
23. Bellenger NG, Davies LC, Francis JM, et al. Reduction in sample size for studies of remodeling in heart failure by the use of cardiovascular magnetic resonance J Cardiovasc Magn Reson 2000;2;271–278.
24. Packer M, Antonopoulos GV, Berlin JA, et al. Comparative effects of carvedilol and metoprolol on left ventricular ejection fraction in heart failure: results of a meta-analysis. Am Heart J 2001;141:899–907.
25. Nayak KS, Pauly J, Nishimura DG, et al. Rapid ventricular assessment using real-time interactive multislice MRI. Magn Reson Med 2001;45:371–375.